Settling dynamics of cohesive sediments in a highly turbid tidal river

Sophie Defontaine, Isabel Jalón-Rojas, Aldo Sottolichio, Nicolas Gratiot, Cédric Legout

Settling dynamics of cohesive sediments in a highly turbid tidal river

Sophie Defontaine [(1)], Isabel Jalon-Rojas [(1)], Aldo Sottolichio [(1)], Nicolas Gratiot [(2)], Cédric Legout [(2)]

[(1)] *Univ. Bordeaux, CNRS, Bordeaux INP, EPOC, UMR 5805, F-33600 Pessac, France*
[(2)] *Univ. Grenoble Alpes, CNRS, IRD, Grenoble INP, IGE, 38000 Grenoble, France*

Abstract

An optical settling column was used in the Garonne Tidal River to estimate the settling velocity of suspended matter in surface waters over a period characterized by contrasting hydrological conditions. A time and space variability of settling velocity was observed during this study. The settling velocities of surface suspended matter ranged from 0.018 to 0.268 $mm.s^{-1}$, and the median diameter of dispersed particles varied from 4.74 to 14.38 μm. The data revealed the physical processes influencing the sediment settling dynamics throughout different time scales in a highly turbid tidal river. On tidal and fortnightly time scales, resuspension, deposition and advection mechanisms were the major drivers of the settling velocity variability, while it is likely that the estuarine turbidity maxima (ETM) was responsible for seasonal variations. The findings of this work suggest that in tidal rivers, salinity is too low to promote flocculation, whereas ETM can play a key role in enhancing this process. The stronger variability in settling velocity occurs on a tidal timescale, with median values up to four times higher at the end of the ebb tide than at high water. These variations cannot be correlated to salinity or sediment concentration. On a seasonal timescale, flocculation appears to be strongly correlated with the presence of the ETM and associated fluid mud layer. A simple correlation based on tidal variations seems to be a better predictor than the relationships based on the sediment concentration.

Keywords: sediment dynamics, settling velocity, cohesive sediment, ETM, SCAF, tidal river

1. Introduction

The accumulation of cohesive sediments is one of the most prominent issues in many tidal estuaries, as it has major implications on estuarine morphodynamics and on water quality and dredging strategies to support harbor activities. Cohesive sediments have the ability to aggregate into flocs, which drastically affects sediment dynamics (Manning et al., 2010; Mehta, 2013; whitehouse, 2000; Winterwerp, 2002; Xu et al., 2010). The settling velocity of flocs can be a couple of orders of magnitude larger than that of primary particles. In this sense, flocculation largely influences fine-grained sediment transport through increased settling velocity and hindered settling, resulting in stronger deposition and promoting the formation of estuarine turbidity maxima (ETM) (Burchard et al., 2018; Horemans et al., 2020; Winterwerp, 2002). The strong cohesiveness of aggregated sediments due to organic content may also reduce bed sediment erodibility (Malarkey et al., 2015; Parsons et al., 2016). Factors enhancing flocculation include salinity (Gibbs, 1983; Liu et al., 2018; Mietta et al., 2009; Zhang et al., 2021), the suspended sediment concentration (Mikkelsen and Pejrup, 1998; Verney et al., 2009), biological processes (Eisma, 1986; Deng et al., 2021; Fall et al., 2021; Furukawa et al., 2014) and the turbulent characteristics of the flow (Gratiot and Manning, 2004; Mikes et al., 2004; Verney et al., 2011; Winterwerp, 2002).

The effects of flocculation on sediment settling dynamics and deposition processes are highly affected by hydrological conditions and may thus vary over different time scales. Settling variations over the semidiurnal tidal cycle and the fortnightly cycle have been reported up to one or two orders of magnitude (Guo et al., 2017; Pejrup and Mikkelsen, 2010; van Leussen, 1999; Van der Lee, 2000; Manning et al., 2006). On a seasonal timescale, river runoff drives salinity intrusion, the rate of organic matter and suspended matter concentration, resulting in seasonal variation in settling velocities (Xia et al., 2004). In addition, settling velocity is challenging to study experimentally due to the fragile nature of flocs.

The most used techniques in recent decades have been settling tubes, such as Owen tubes (Owen, 1971). Although settling columns are inexpensive and easy to deploy in highly turbid environments, they also have many disadvantages, such as (1) they may destroy larger flocs during sampling (Dyer et al., 1996; Eisma et al., 1991), (2) flocculation due to differential settling may occur in the tube (Eisma, 1986), (3) subsampling contamination due to incomplete removal of fine-grained sediment and (4) changes in temperature may generate convection inside the tube (Puls and Kühl, 1996). Since then, new settling columns have been developed to overcome these inconveniences, with sidewall withdrawal tubes to avoid subsampling contamination, thermal insulation and autonomous sampling systems (Cornelisse, 1996; van Leussen, 1996). The Sedigraph instrument also measures the settling velocity of fine grain sediment, however it is designed for laboratory granulometric analyses and too-high concentrations required for such analyses may lead to hindered settling effects and the underestimation of settling velocities (Stein, 1985).

Recently, considerable improvements have been made in settling velocity measurement, and various in-situ instruments have been developed based on optic (Kineke et al., 1989; Gratiot et al., 2015; Murray et al., 1996; Zaneveld et al., 1982), video (Fennessy et al., 1994; Heffler et al., 1991; Sanford et al., 2005; Smith and Friedrichs, 2011; Sternberg et al., 1996; Van Leussen and Cornelisse, 1993), holographic (SEQUOIA; Graham and Nimmo Smith, 2010; Owen and Zozulya, 2000; Watson et al., 1998, 2004) and laser (Agrawal and Pottsmith, 2000; Mikkelsen and Pejrup, 2001) methods among others (Mantovanelli, 2005). The advantage of these new techniques is that they additionally

provide floc size information. A laser-based instrument is an indirect method of estimating settling velocity, as it uses scattering theory for regularly shaped spherical particles to estimate particle sizes and then computes the in situ mean effective density and mean settling velocity (Mikkelsen and Pejrup, 2001). Such methods may induce error when nonspherical particles are studied. Video and holographic-based methods can simultaneously measure particle size and settling velocity in a fully automated manner (Graham and Nimmo Smith, 2010; Manning and Schoellhamer, 2013). The density may then be estimated with the Stokes equation, giving additional information on the particles inside the water column. Major limitations of such methods are the heavy time cost of data postprocessing, the complex deployment of an imposing structure, a unique positioning close to the seabed, and a range of application limited by a concentration lower than a few grams per liter for the most advanced ones (Fennessy et al., 1994; Owen, 1971). Indeed, holographic systems are generally limited to concentrations smaller than tens of $mg.L^{-1}$ (SEQUOIA), laser instruments are capable of being used up to 800 $mg.L^{-1}$ (Mikkelsen and Pejrup, 2001), Owen tubes are appropriate for use up to 5 $g.L^{-1}$ (Owen, 1971), and one of the most advanced methods found in the literature is the INSSEV system, which is able to function with concentrations up to 8.5 $g.L^{-1}$ (Fennessy et al., 1994). However, the INSSEV must be positioned close to the seabed. A comprehensive review of the different techniques, their advantages and disadvantages was proposed by Mantovanelli and Ridd (2006) and pursued by Wendling et al. (2015).

In the highly turbid Garonne Tidal River, the surface concentration may reach 7 $g.L^{-1}$ and tens of grams per liter close to the riverbed. Recently, an optical settling column was specially designed for this type of hyper turbid environment, namely, the System for the Characterization of Aggregates and Flocs (SCAF) (Wendling et al., 2015; Gratiot et al., 2015). The SCAF was successfully used under laboratory conditions for a wide range of natural sediment concentrations (20-30,000 $mg.L^{-1}$; Le et al. (2020)). It was also used in the field during reservoir flushing in the Arc River in the Alps (Legout et al., 2018). This new instrument benefits from easy handling and straightforward data postprocessing. However, this new patented equipment has never been used in the field in a hyperturbid environment that is subjected to tidal forcing.

Understanding and predicting settling and deposition processes is a key factor to achieve realistic simulations of suspended sediment fluxes and concentration (Diaz et al., 2020; van Maanen and Sottolichio, 2018). Various theoretical (process-based or empirical) formulations for predicting settling velocities have been developed. A power law relating the settling velocity to SSC below the hindered settling regime has been outlined by various authors (Dyer et al., 1996; Jones and Jago, 1996; Pejrup and Edelvang, 1996; Puls et al., 1988). This type of formulation was based on the hypothesis that SSC is the driving parameter of flocculation, and therefore on the settling velocity variation. Van der Lee (2000) reported that the variations in settling velocity were related to the tidal phase in the Dollard Estuary and proposed a formulation based on the time from high water. Further investigations highlighted the dominant role of turbulence-induced aggregation and floc breakup processes in settling velocity variations (Spearman et al., 2011). For example, Verney et al. (2011) confirmed the major dependency of floc sizes on the Kolmogorov microscale. Other studies defined a shear stress parameter that is included in the formulation of the settling velocity to consider the influence of the turbulence (Dyer and Manning, 1999; Manning et al., 2007; Pejrup and Mikkelsen, 2010; Winterwerp et al., 2006). However, studies on the settling dynamics of cohesive sediments in tidal rivers, which are barely affected by salinity, therefore characterized

by less favorable flocculation conditions, are rare.

The aim of this study is to explore the variability of the settling velocity along different time scales in a tidal river that is characterized by low salinity and low rate of organic matter and to investigate simple empirical formulations of the settling velocity, which are necessary for numerical modeling purposes. A series of field measurements have been conducted in the Garonne Tidal River (Gironde Estuary, France). A specific protocol was designed to use the SCAF device in a highly turbid river subjected to semidiurnal tidal forcing. This new instrument allowed us to evaluate for the first time the values of settling velocities and their variations over different time scales in such environment. The role of the ETM in those variations is discussed, and different empirical formulations are proposed to predict the settling velocity variations observed in the Garonne Tidal River.

2. Study site

The Garonne Tidal River is one of the two tributaries of the Gironde Estuary located on the southwest coast of France (Fig. 1). From the confluence with the Dordogne River to the tidal intrusion limit, the Garonne Tidal River extends over 95 km. The Garonne tidal river is subjected to a semidiurnal macrotidal forcing, with a tidal amplitude ranging from 1.7 m to 6.2 m at the confluence (Jalón-Rojas et al., 2018). In addition, during its propagation into the tidal river, the tidal wave becomes asymmetric with shorter (longer) flood (ebb) duration and stronger (weaker) flood (ebb) currents. This hypersynchronous behavior results in intense tidal pumping, leading to massive sediment trapping and a highly concentrated ETM (Allen et al., 1980). During periods of low river discharge, the suspended matter is advected landward into both tidal rivers. In the Garonne Tidal River (GTR), a large ETM occurs at river flows lower than 300 $m3.s^{-1}$, with surface concentrations of few grams per liter (Jalón-Rojas et al., 2015, 2021).

Little is known regarding the floc size distribution or settling velocity of suspended sediment in the Garonne Tidal River, as most of the previous studies were focused on the downstream part of the Gironde Estuary, which is mainly composed of a mud-sand mixture (Allen, 1971; Manning et al., 2004; Sottolichio et al., 2011). Gibbs et al. (1989) showed a progressive increase in the mean diameter of suspended sediment particles from the Garonne Tidal River to the mouth of the Gironde Estuary. According to this study, the mean diameter ranges from 5 μm to 20 μm in the Garonne Tidal River, and a floc size maximum is reached 30 km seaward from the ETM (i.e., close to the mouth of the estuary). More recent studies have shown that sediment in the Gironde Estuary is characterized by low organic content with no seasonal variation (Abril et al., 2002; Etcheber et al., 2007).

The Garonne Tidal River is therefore characterized by a pronounced and well-documented estuarine turbidity maxima largely stretching in fresh waters during the dry season. Such highly concentrated ETM occurs in a region barely affected by salinity and variation in organic content and where no settling velocity data are available, which makes this system an ideal site for this study. Although different process-based models of the Gironde Estuary and the Garonne Tidal River have been developed over the past decades, all of which adequately reproduce the ETM in the lower estuary, they still face challenges in reproducing the realistic SSC in tidal rivers (Diaz et al., 2020; Lajaunie-Salla et al., 2017; van Maanen and Sottolichio, 2018). Such models were based

on a strong hypothesis on the settling velocity and did not rely on in situ measurements in the tidal river.

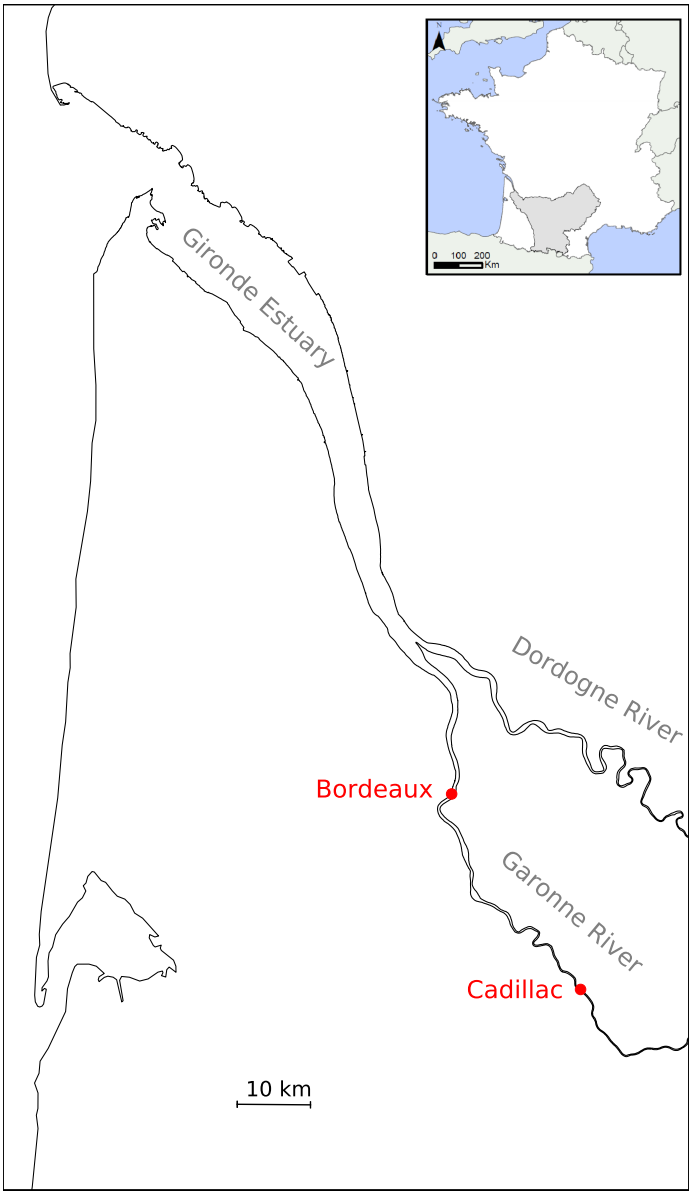

Figure 1: Map of the Gironde Estuary and the Dordogne and Garonne Tidal Rivers with locations of the field measurement sites (Bordeaux and Cadillac).

3. Materials and Methods

3.1. Laboratory experiments

The SCAF device was developed by the French Institute of Environmental Geosciences to efficiently measure the sediment settling velocity in a highly turbid environment (Wendling et al., 2015; Gratiot et al., 2015). This settling column is equipped with 16 infrared emitters and 16 diametrically opposed photosensors. It measures the variation in light attenuation with time and depth

to estimate the settling velocity of suspended sediments, based on the fact that the absorbance $A = -log(I/Imax)$ of a suspension of particles is the sum of the individual absorbance of each particle, where I is the light intensity and Imax the light intensity through clear water. During the settling, particles with the highest settling velocity will progressively fall below a given level, leading to a progressive decrease of the absorbance. The settling velocity of each particle size class is then given by the slope of a specific iso-absorbance value in a depth-time graph. The post-processing is adapted from the method proposed by Piro et al. (2011). A more complete description of the measurement principle can be found in Wendling (2015) and Gratiot et al. (2015).

The SCAF estimates a flocculation index (FI) as follow: $FI = (w_b - w_s)/w_s$, where w_b is the settling velocity measured with six lower IR sensors of the settling column and ws is the settling velocity with six upper IR sensors of the settling column. In case of non-cohesive sediments, the slope of iso-absorbances with time is constant along the depth of the settling column, meaning w_b is equal to w_s and so FI is zero. For cohesive sediments, flocculation may occur during settling resulting in an increased settling velocity with depth and time, leading to w_b greater than w_s and FI greater to 0. The FI values reported in previous studies typically range from 0 to 10 (Wendling, 2015; Le et al., 2020; Legout et al., 2018). Negative values of FI could be due to hindered settling effects.

Prior to field measurements, different tests were conducted in the laboratory to design an experimental protocol adapted to the use of the SCAF in a turbid environment subjected to tidal forcing.

Even though the SCAF was previously used successfully with highly concentrated suspensions, up to 30 $g.L^{-1}$ (Le et al., 2020), the range of concentrations in which the instrument is able to measure the settling velocity may be highly dependent on the mud composition. Therefore, we tested the SCAF with 7 suspensions of different concentrations ranging from 0.2 to 15 $g.L^{-1}$ prepared with natural mud from the Garonne Tidal River. Only for the two more concentrated suspensions (10 $g.L^{-1}$ and 15 $g.L^{-1}$) were the sensors saturated during the first few seconds of measurement (9 and 28 seconds, respectively). These laboratory tests validated the use of the SCAF for settling measurements of surface waters in the Garonne Tidal River, knowing that the surface concentration value of 15 $g.L^{-1}$ is much higher than the surface concentration reported in the literature thus far (Sottolichio and Castaing, 1999; Jalón Rojas, 2016).

The second limiting factor in designing our protocol was the settling time: the longer the water sample is allowed into the settling column, the wider the range of particles considered in the median settling velocity estimation. Previous studies using the SCAF selected settling times of 5 h or more to catch the settling of very fine particles (Legout et al., 2018). Such a long settling time was not appropriate to study variations throughout the semidiurnal tidal cycle. This limitation is compounded by tidal asymmetry, which triggers very short flood periods in the Garonne Tidal River (up to 4 h at Bordeaux station during spring tides). Therefore, we carried out settling tests of different duration, namely, 1 h, 1 h30, 2 h, 2 h30 and 3 h, to determine the optimal time resolution. Figure 2 presents the settling velocity distributions for the five experiments where the settling time varies from 1 h to 3 h. Our results demonstrate that the median and quartile values were very similar for all experiments, with median settling velocity values ranging from 0.068 to 0.073 $mm.s^{-1}$. The minimum settling velocity decreased with increasing settling time, as expected. Thus, we decided to consider a settling time of 1 h 30 h to be able to collect water samples at least

every two hours. This sampling interval allowed us to catch the main stages of the semidiurnal tidal cycle: low water, mid-flood, high water and mid-ebb, even when the tide is strongly asymmetric with a flood duration of 4 hours.

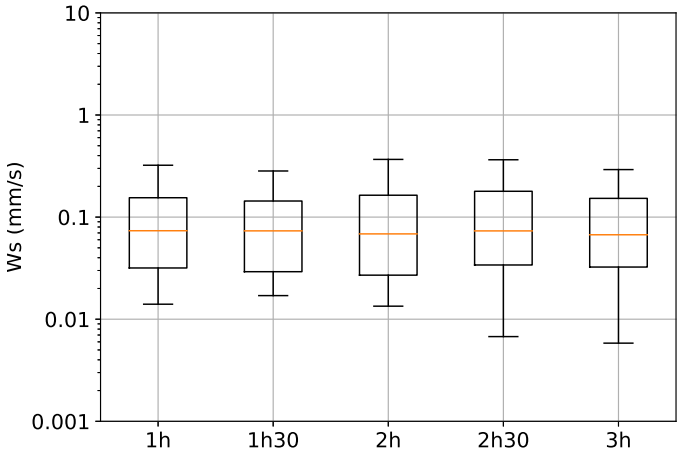

Figure 2: Distribution of the settling velocity for the five settling time tests under laboratory conditions

3.2. Field campaigns

Nine field campaigns were carried out in the Garonne Tidal River to evaluate the variations in sediment settling velocities in surface waters over different time scales (tidal cycle, fortnightly cycle, spring-to-summer transition). A summary of the tidal range and river flow conditions during the field experiments are given in Table 1. Figure 3 shows timeseries of (a) water elevation at Bordeaux and Cadillac and (b) daily averaged river flow at Tonneins (i.e., first station upstream of the tidal propagation limit) with shadowed areas representing the presence of the ETM at Bordeaux (gray) and Cadillac (blue).

Table 1: Experimental conditions

Location	Date	Tidal range (m)	River Flow ($m^3.s^{-1}$)	SSC ($g.L^{-1}$)
Fixed station				
Bordeaux	May 18th, 2021	3.9	680-770	0.53
	May 25th, 2021	5.10	350-420	2.07
	June 24th, 2021	5.15	250-300	4.16
	July 5th, 2021	3.9	230-300	2.24
	August 25th, 2021	5.10	120	7.80
	August 30th, 2021	3.6	85	4.64
Cadillac	June 25th, 2021	5.25	270-330	0.18
	July 2nd, 2021	3.9	230-260	0.04
	August 23rd, 2021	5.15	100	2.07
Longitudinal sections				
From Bordeaux to Cadillac	May 24th, 2021	5.1	390-440	
	June 18th, 2021	4.25	140-160	
	July 19th, 2021	4.15	215-240	
	August 19th, 2021	4.1	105	

Field measurements were conducted in two different locations, at Bordeaux and Cadillac (Fig.1), located 25 and 62 km from the river confluence, respectively, and 95 km and 132 km from the mouth, respectively. At these locations, water levels and surface turbidity are continuously recorded by automatic networks, allowing the monitoring of the upstream shift of the ETM during the whole period (https://data.shom.fr et https://magest.oasu.u-bordeaux.fr/). In addition, the tidal wave reaches its maximum amplitude along the estuary between these two stations (Bonneton et al., 2015). The measurements took place at Bordeaux on May 18th and 25th, 2021, on June 24th, 2021, on July 05th, 2021 and on August 25th and 30th, 2021, and at Cadillac on June 25th, 2021, on July 2nd, 2021, and on August 23rd, 2021 (Tab.1). This period corresponds to the spring-to-summer transition, when the ETM shifts from the lower estuary toward the tidal rivers because the river flow decreases to its minimum annual value (Fig. 3). At both stations, vertical profiles of velocity, salinity, temperature and turbidity were measured. Velocity profiles were continuously recorded at 4 Hz by a Nortek Signature 500 kHz ADCP, with a vertical resolution of 0.5 m. Velocity profiles were then averaged over 10 min intervals. Salinity, temperature and turbidity profiles were recorded every 30 min with an NKE MPx multiparameter probe. This optical turbidity sensor was calibrated in the laboratory with sediments from the Garonne River to deduce the suspended sediment concentration (SSC). Calibration relationships are known to change with floc characteristics such as particle size, density and composition (Boss et al., 2009; Downing, 2006; Druine et al., 2018). Filtration was conducted in the field to estimate the SSC of surface waters every hour. These field SSC measurements satisfactorily fitted the laboratory calibration used to convert turbidity data. Some of these samples were also used to estimate the settling velocity with the SCAF at approximately high water, high water + 2 hrs, high water + 5 hrs, low water and low water +2 hrs.

During boat surveys along the GTR between Bordeaux and Cadillac on May 24th, 2021, June 18th, 2021, July 19th, 2021 and August 19th, 2021 complementary bed sediment samplings were carried out with a Berthois cone, which is a weighted metallic cone that is dragged with a rope at the rear of the boat.

Dispersed particle size distributions (PSDs) of the sediments used in the settling column and riverbed sediments were measured after 60 seconds of stirring and sonication at their maximum level with a Malvern laser-diffraction instrument operating in the range 0.01-2000 μm.

3.3. Data bases

The daily river discharge for the Garonne River at Tonneins station and the water elevation at Cadillac were retrieved from the Banque Hydro database (www.hydro.eaufrance.fr). The water elevation at Bordeaux was extracted from the SHOM database (www.data.shom.fr/).

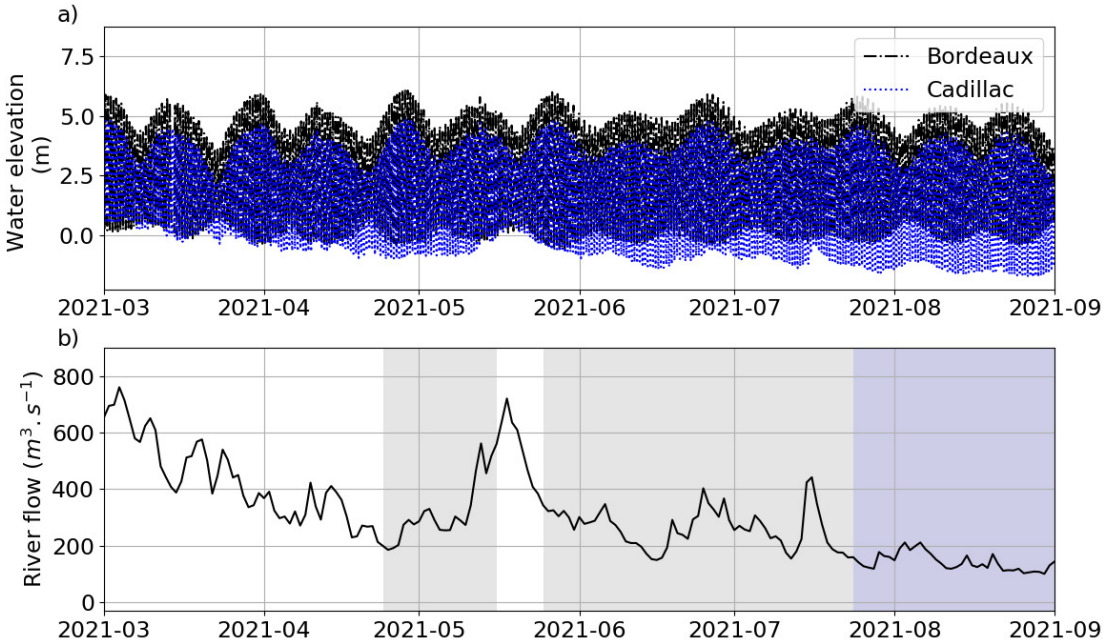

Figure 3: Time series of a) water elevation (m) at Bordeaux and Cadillac and b) daily averaged river flow ($m^3.s^{-1}$) at Tonneins. The shadowed areas correspond to the presence of the ETM at Bordeaux (gray) and Cadillac (blue).

4. Results

This section presents the observations of sediment settling dynamics in the surface waters of the Garonne Tidal River over different time scales. First, variations along the semidiurnal tidal cycle are presented, and then the data collected during neap and spring tides are compared. Finally, variations over the spring-to-summer transition are investigated. In this study, the settling velocity of suspended sediment is expressed as the median settling velocity w_{50}, and the median diameter D50 values refer to the dispersed particles (after sonication). The velocity data are projected into a local coordinate system with the x-axis directed along the riverine channel with positive values for inflow, the y-axis directed laterally toward the right bank, and the z-axis directed upward. The

velocities shown in the figures refer to the velocity component along the channel axis (x-axis). Most of the data presented in this section were collected at Bordeaux. Data collected at Cadillac were mostly not representative due to a very low SSC (below 60 $mg.L^{-1}$), i.e., out of the concentration range of the SCAF and the Malvern instruments. Only seven samples appeared to be significant (five of which are presented in Figure 5), and they are discussed in subsection 5.2.

4.1. Variations throughout the semidiurnal tidal cycle

Over the complete set of data, the settling velocity ranged from 0.018 to 0.268 $mm.s^{-1}$, and the median diameter ranged from 4.74 to 14.38 μm. Settling velocities were lower at Bordeaux than at Cadillac, with values ranging from 0.018 to 0.144 $mm.s^{-1}$ and from 0.067 to 0.268 $mm.s^{-1}$, respectively. Median diameters were higher at Cadillac than at Bordeaux, with average values of 11.62 and 7.17 μm, respectively. Two examples of data collected along a tidal cycle at Bordeaux and Cadillac are presented in Figures 4 and 5, with timeseries of (a) water level in meters, profiles of (b) velocity, (c) suspended sediment concentration and (d) salinity, median diameter of dispersed particles from surface waters and settling velocity of suspended sediments from surface waters. A distinct pattern was observed at Bordeaux along every tidal cycle, with a decreasing settling velocity during the rising tide and an increasing settling velocity during the falling tide (Fig. 4 f). The range of settling velocity (i.e., quartile values) also varied during the tidal cycle, with a wider range at the end of the ebb and a narrower range at the end of the flood. A similar pattern was found for the median diameter. At Cadillac, the pattern was flattened compared to Bordeaux, with relatively similar settling velocities from mid-flood to mid-ebb and an increase at the end of the ebb (Fig. 5 f).

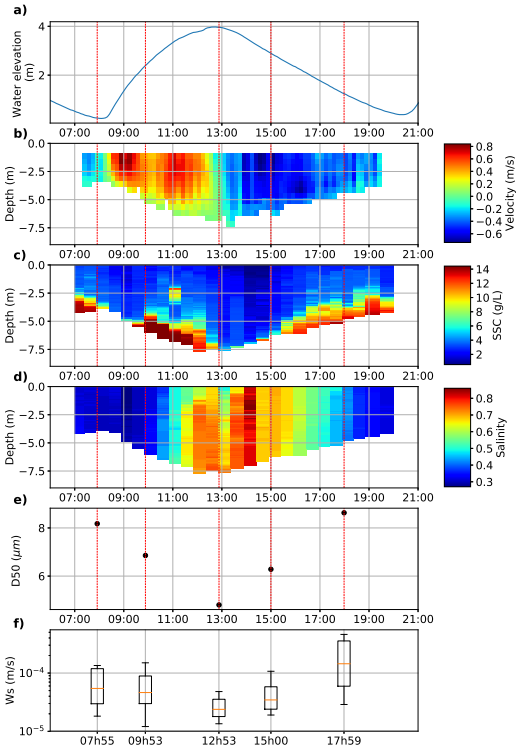

Figure 4: Time series of a) water elevation in meters, b) velocity profiles in meters per second, c) suspended sediment concentration in grams per liter, d) salinity, e) median diameter of surface suspended sediments in microns, and f) settling velocity distribution of surface suspended sediments in meters per second. Data collected at Bordeaux on August 30th.

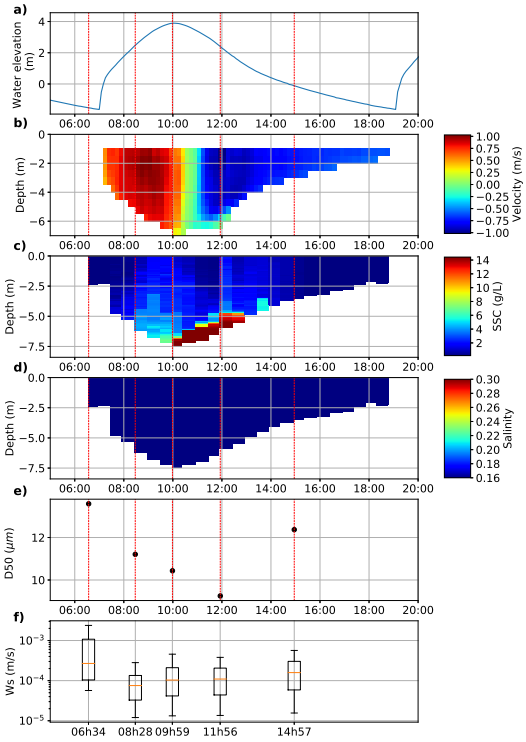

Figure 5: Time series of a) water elevation in meters, b) velocity profiles in meters per second, c) suspended sediment concentration in grams per liter, d) salinity, e) median diameter of surface suspended sediments in microns, and f) settling velocity distribution of surface suspended sediments in meters per second. Data collected at Cadillac on August 23rd.

This tidal pattern suggests that sediment processes and transport mechanisms taking place along the tidal cycle, such as erosion, deposition and advection, determine the settling velocity and the median diameter. To precisely distinguish advection from local vertical processes (erosion and deposition), simultaneous measurements at two close stations are needed. However, the evolution of the median settling velocity along with the depth-averaged SSC and velocity (Fig. 6) provides insight into the processes involved. Throughout the tidal cycle, the variation in SSC with flow velocity at Bordeaux displayed the same specific pattern for all hydrological conditions. At the end of the outflow, the decrease in SSC associated with a decrease in velocity indicates a deposition mechanism (1). The deposition lasted from the beginning of the inflow until a velocity of approximately 0.4 $m.s^{-1}$ was reached. Then, the increasing velocity increased with an increase in SSC, suggesting resuspension (2). Another phase of decreasing SSC and velocity evokes deposition (3). When the outflow reached -0.4 $m.s^{-1}$, both SSC and velocity increased again, probably due to resuspension (4). At the end of the outflow, the SSC increased or remained equal while the velocity decreased, which is likely associated with advection and/or diffusion mechanisms (5). The associated patterns of settling velocity revealed that it was higher at the end of the resuspension/advection/diffusion phases and lower at the end of the deposition phases. Higher values of settling velocity at the

end of resuspension phases could be attributed to bigger particles being eroded from the bed and maintained in suspension by higher turbulence and/or higher flocculation promoted by higher SSC. In the other hand, lower value during high water slack time may be attributed to sorting processes due to lower turbulence and so deposition of the bigger particles.

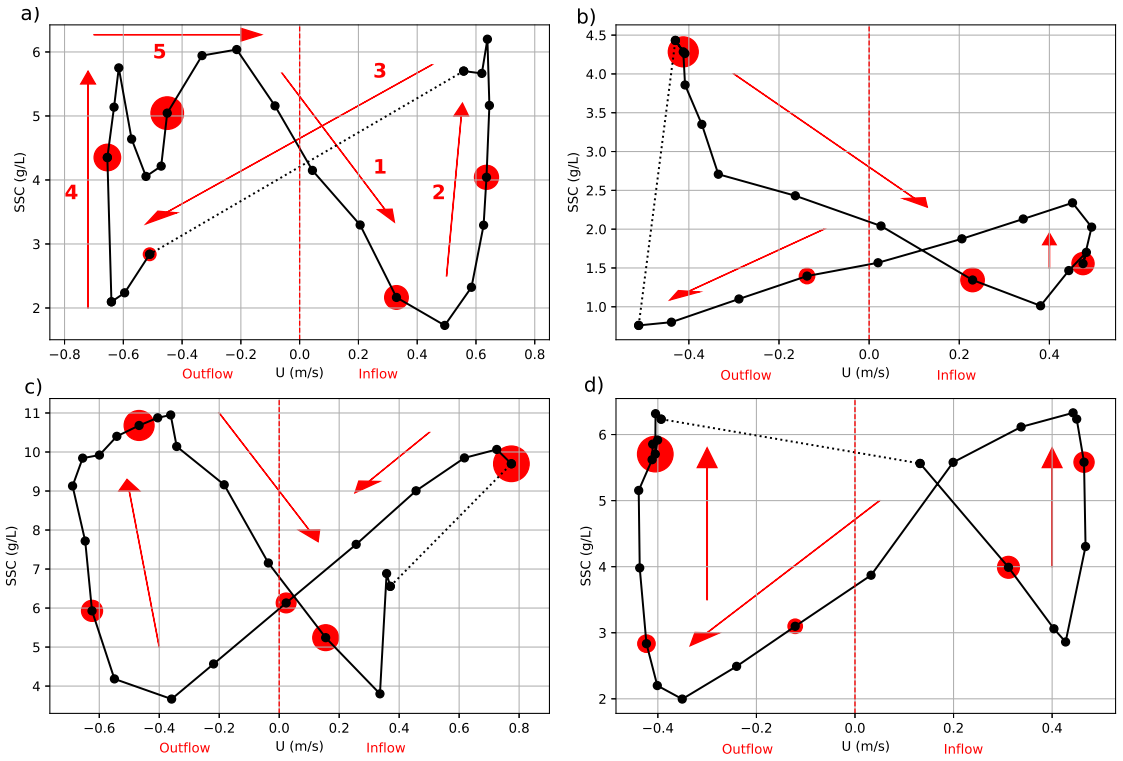

Figure 6: Variation in the depth-averaged SSC with the depth-averaged velocity for the data collected at Bordeaux on a) June 24th, b) July 5th, c) August 25th and d) August 30th. The red dot size represents the relative order of magnitude of the median settling velocity of surface suspended sediment.

4.2. Variations throughout the fortnightly cycle

Even if the settling velocity followed the same pattern along the tidal cycle for all the measurement conditions, differences can be observed when we discriminate neap tide from spring tide observations. Figure 7 shows the variations in the settling velocity distribution of surface sediments in relation to the time to high water for (a) spring and (b) neap tides. The median settling velocity was slightly higher during spring tides than during neap tides, with mean values of 0.072 $mm.s^{-1}$ and 0.06 $mm.s^{-1}$, respectively. The range of settling velocity was also wider during spring than during neap tide. This is likely the result of higher resuspension and vertical mixing during spring tide, as revealed by the higher SSC and tidal currents in spring (Fig.6 a and c) than at neap tides (Fig.6 b and d). Regarding the median diameter, the comparison between neap and spring tide is not straightforward. Similar values of D50 were observed in July for both conditions. In May, the median diameter during neap tide was slightly larger than during spring tide, with mean values of 12.25 μm and 10.66 μm, respectively, while in August, the opposite trend was observed, with mean values of 6.95 μm and 8.25 μm, respectively. This pattern may be explained by the river flood (approximately 700 $m^3.s^{-1}$, Fig. 3) that occurred in May at neap tide, which might have brought

297 some particles with higher dispersed D50 from landward sources.

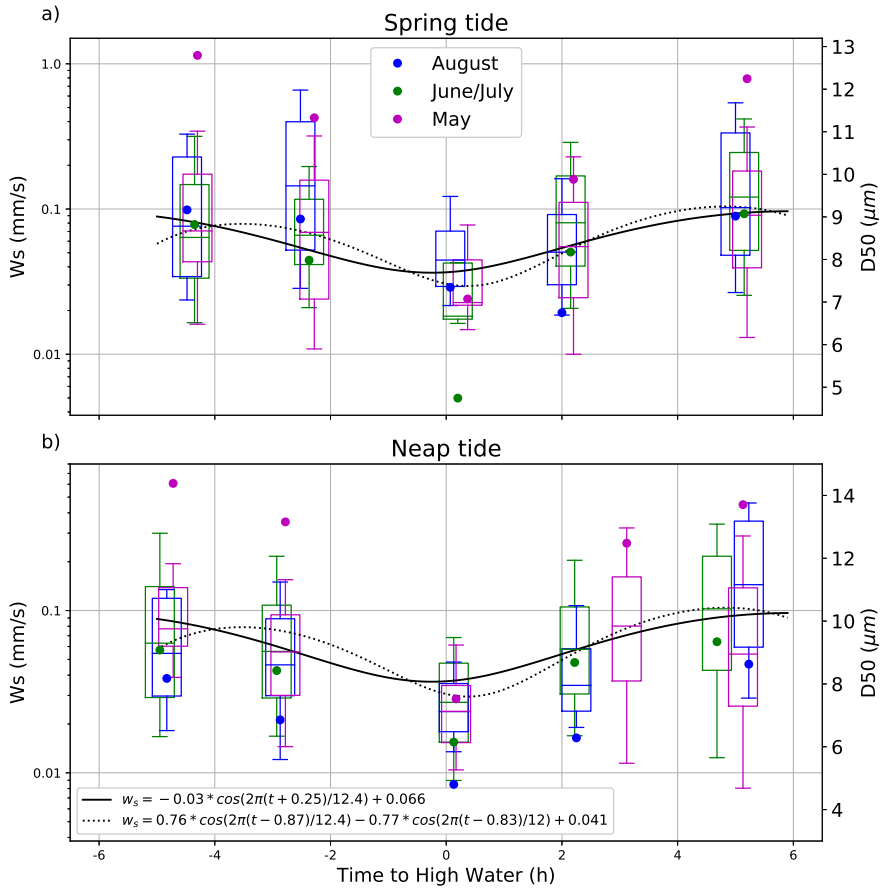

Figure 7: Settling velocity distribution in millimeters per second (colored box plots) and median diameter in microns (colored dots) of surface suspended sediments as a function of the time to high water during a) spring tides and b) neap tides. Data presented in this figure have been collected at Bordeaux. The colors correspond to the period of measurement: magenta for May, green for the end of June and the beginning of July and blue for August. The full and dotted black lines represent two relations of the median settling velocity variation with the time to high water, which are discussed in Section 5.2.

298 *4.3. Seasonal variations*

299 Observations were carried out during four consecutive months to study the variations in sediment
300 settling dynamics during the transition period of decreasing river flow that promotes the shift of
301 the ETM from the lower estuary to the tidal river. In May, the river flow was impacted by a spring
302 freshet, while it decreased in the following months to less than 200 $m^3.s^{-1}$ in August (Fig. 3).
303 The settling velocities slightly increased between May and August, with tidally averaged settling
304 velocities of 0.059 and 0.072 $mm.s^{-1}$, respectively (Fig. 7). Note that the increase between May
305 and August was more pronounced at spring tides than at neap tides. This enhanced increase during
306 spring tide might be due to higher resuspension and vertical mixing in August due to higher tidal
307 current intensity and/or more available sediment on the bed.

308 In Figure 7, in contrast to the increase in settling velocity, a decrease in the median diameter of
309 the dispersed particles can be observed between May and August, with tidally averaged D50 values

of 11.5 and 7.6 μm, respectively. This tendency is even clearer in Figure 8, which represents the particle size distribution of dispersed particles collected in surface waters at Bordeaux in the same period. A clear shift of the particle size distribution can be noticed between May (in blue) and the following months (in red and black). In July, after the installation of the ETM (see discussion in Section 5), the quantity of small particles (< 10 μm) increased, and the second tiny peak at approximately 500 μm (sand fraction) flattened.

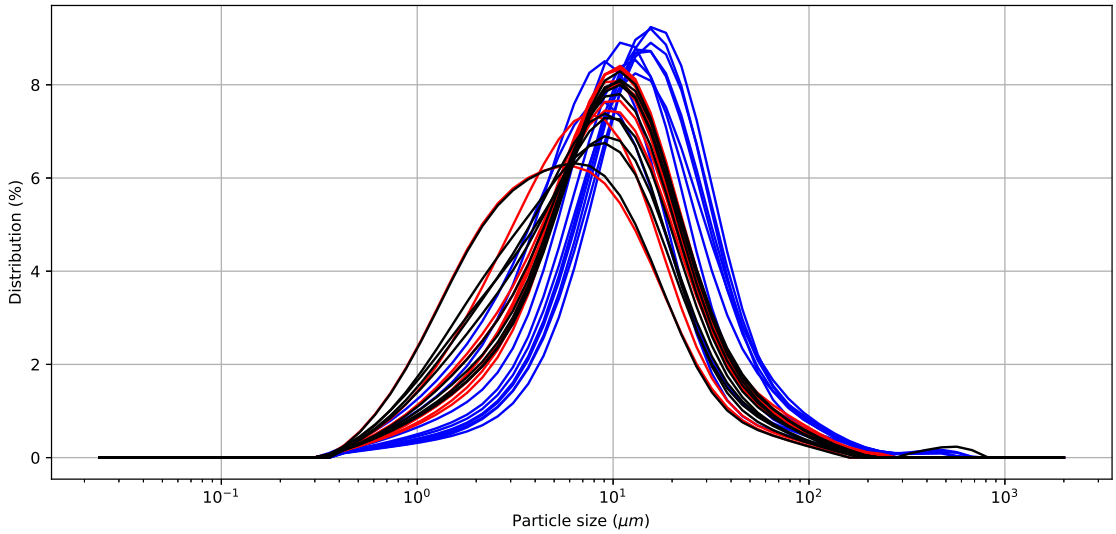

Figure 8: Particle size distribution of the dispersed surface particles collected in May (blue), June and July (red) and August (black) at Bordeaux.

5. Discussion

5.1. Influence of the ETM

The influence of the upward displacement of the ETM into the Garonne Tidal River on settling dynamics was evaluated through field measurements carried out in late spring and the beginning of summer (Fig. 3). As expected, the ETM progressively moved upward from the Gironde Estuary to the Garonne Tidal River with decreasing river flow: (1) in April, the river flow decreased to 200 $m^3.s^{-1}$, and the ETM appeared in Bordeaux; (2) in May, a freshet (Q = 700 $m^3.s^{-1}$) momentarily moved the ETM downward, which moved back to Bordeaux in June; and (3) the ETM finally reached Portets and Cadillac in July (Fig. 3). In the Gironde Estuary, the ETM is associated with the presence of a fluid mud layer at the bottom. During the dry season, when the river flow is lower than 500 $m^3.s^{-1}$, ETM moves upstream, and fluid mud forms in the tidal rivers (Sottolichio and Castaing, 1999). The variation in the particle size distribution of bed sediments along the Garonne Tidal River for different river flow conditions is shown in figure 9. Bed sediment samplings carried out between May and August 2021 (Fig. 9) seem to confirm the formation of fluid mud in the Garonne Tidal River with decreasing river flow. In May, the bed surface of the GTR is composed of mud, sand and pebbles/rocks depending on location, while in June, the GTR is mostly covered by mud. In July, a slight increase in river flow was sufficient to remove some patches of mud (at km 12 and km 23). In August, the river flow lowered to 100 $m^3.s^{-1}$, and a fluid mud layer covered

almost the entire portion between Bordeaux and Cadillac. The shift in the particle size distribution observed between May and the following months (Fig. 8) was likely induced by the displacement of the ETM and the arrival of a fluid mud layer on the bed of the Garonne River.

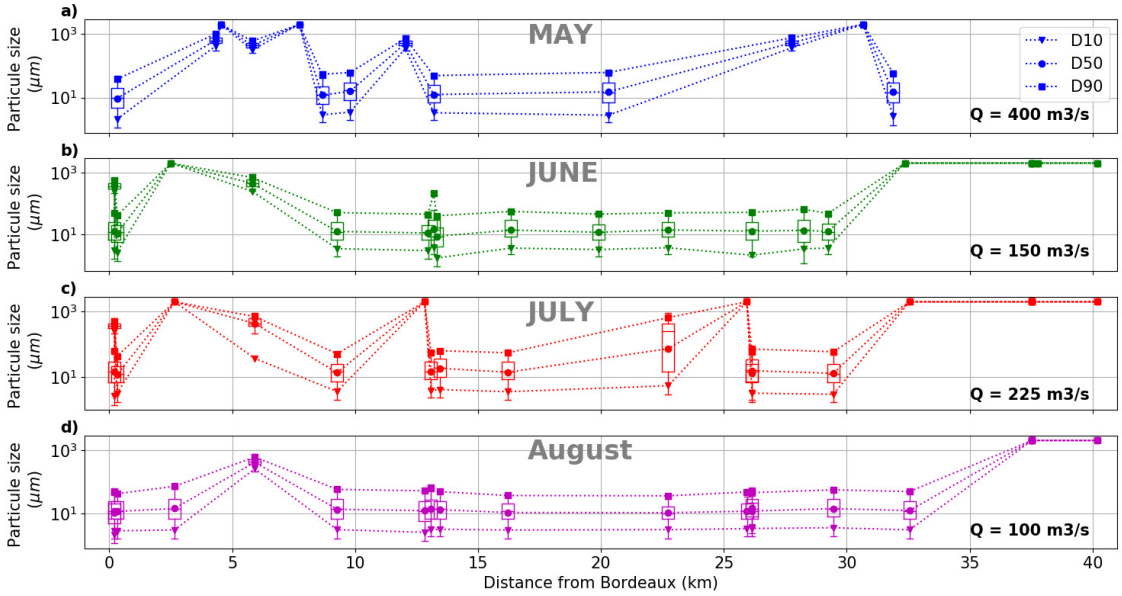

Figure 9: Particle size distributions of bed sediments along the Garonne Tidal River: from Bordeaux to Cadillac.

The increase in settling velocity when the median diameter of dispersed particles decreases may indicate higher flocculation of particles. In Figure 10, the flocculation index (FI), which indicates the tendency of sediments to flocculate in quiescent water (i.e., in the settling column) is represented as a function of SSC. The flocculation appeared to be strongly correlated with the SSC, with a linear increase in FI with SSC. In May (before ETM arrival in Bordeaux), the SSC is reduced, as is the FI, with a mean value of 1.34. In August (after ETM installation in Bordeaux), the SSC increased, and the FI varied from 2 to 12, with a mean value of 5.8 (Fig. 10). The settling velocity variations seemed also correlated with the FI and SSC, as higher settling velocities were observed at high SSC and FI, and vice versa (Fig. 10 and 12). Therefore, the increase in SSC induced by the upward displacement of the ETM should have favored flocculation and the increase in settling velocities. The influence of SSC on the settling velocity is further detailed in Subsection 5.2.

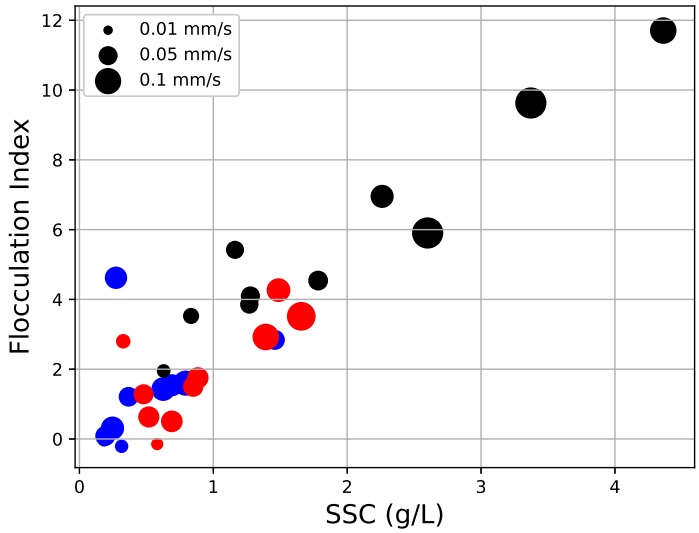

Figure 10: Flocculation index (FI) variations with the surface sediment concentration. Sediments collected in May (blue), June and July (red) and August (black) at Bordeaux. The size of the dot is proportional to the median settling velocity.

In the Garonne Tidal River, the ETM is generated upstream of the salt intrusion limit by tidal pumping during low river discharge (Allen et al., 1980; Jalón-Rojas et al., 2015, 2021). Figure 11 illustrates the median settling velocity of surface sediments as a function of the surface water salinity. In the tidal river where the salinity remained below 0.8, the effect of salinity on suspended sediment dynamics and more precisely on flocculation appeared to be limited. Salinity is well known to promote flocculation in estuaries, whereas in this study, the median settling velocity does not correlate with salinity. This can be partly explained by the fact that higher salinity values are encountered during high water slack times when the deposition process occurs. The deposition process may counteract salinity-induced flocculation in surface waters. Further investigations are needed to more deeply analyze the effects of salinity on flocculation. In the lower Gironde Estuary (i.e., downstream of the salt intrusion limit) salinity may be a key parameter for flocculation and settling dynamics (Gibbs et al., 1989; Mikeš and Manning, 2010). Additional in situ measurements downstream of the lower estuary are required to gain a better understanding of this issue.

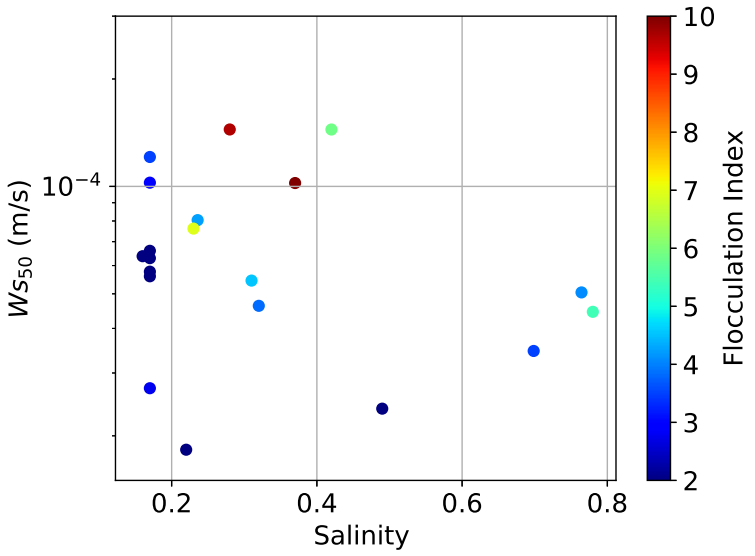

Figure 11: Median settling velocity variations with salinity and flocculation index. Data collected at Bordeaux.

5.2. Settling velocity prediction

The settling process is a key aspect of mud dynamics that depends on the sediment composition, water properties, sediment concentration, and turbulence characteristics of the ambient water, among others. All these parameters vary in time and space. The prediction of settling velocities is therefore challenging, and different complex empirical formulations have been proposed in the literature (Manning and Dyer, 2007; Soulsby et al., 2013). In this section, our results are compared with simple empirical formulations that consider SSC and tidal phase as parameters correlating with the settling velocity. In the absence of any more reliable parameterization, the predictive capabilities of these formulations are assessed, since they are of potential utility for operational simulations.

5.2.1. Relationship with SSC

The settling velocity is supposed to be well correlated with SSC based on the hypothesis that an increase in SSC induces an increase in floc collision frequency, which favors floc growth (Pejrup, 1988). In addition, bed erosion can increase SSC and the resuspension of larger flocs, which could also explain the correlation between SSC and settling velocity. Figure 12 presents the variations in median settling velocity with SSC in surface waters. From those data, a power law relation between the settling velocity and SSC measured at Bordeaux was estimated: $ws = 0.068 * SSC^{0.4}$ (Fig. 12 a). This power law indicated that variations in SSC explained only 41% of the variation in the settling velocity (Tab. 2), which suggests that SSC variations are not sufficient to explain the settling velocity variations. This idea is reinforced by the fact that for similar SSC values, the settling velocities measured in August were lower than those in June/July (Fig. 12 b), whereas the flocculation index was equivalent for both periods (Fig. 10), and the particle size distributions were comparable (Fig. 8).

Figure 12 a) also compares our data with the formulations by Ross (1988) and Mehta (1986) obtained with laboratory experiments. Even if the Ross (1988) formulation gave settling velocities

of the same order of magnitude as the data presented in this study, the influence of SSC on the settling velocity was more important as the slope became steeper. This could be due to differences in sediment and water composition (e.g., binding efficiency, salinity). The hindered regime reached approximately 2 $g.L^{-1}$ in Ross (1988) experiments, while it seems that sediment at Bordeaux did not reach hindered settling at 4 $g.L^{-1}$. Likewise, hindered settling has been shown to start for concentrations greater than 13 $g.L^{-1}$ in the Gironde Estuary Sottolichio et al. (2011). This could mean that flocculation was less important in the Garonne Tidal River than in the study by Ross (1988) .

When data are discriminated by periods of measurement (Fig. 12 b), the covariance between SSC and settling velocity varies on a seasonal time scale. In May, the covariance between the settling velocity and SSC was poor, suggesting that variations in SSC were not significantly driving the variation in settling velocity (Tab. 2). In June/July and August, the slope was steeper, showing a stronger influence of the variations in SSC on the variations in settling velocity, and both parameters were significantly correlated. This reinforces the fact that the ETM installation modified the settling behavior of the particles, as discussed in Subsection 5.1, and SSC had a larger influence on the settling velocity inside the ETM than outside. Similar observations were made in the 'Groot Gat' tidal channel, with varying relations between SSC and settling velocity throughout the seasons (Van der Lee, 2000).

Spatial variability in settling behavior was also observed. The comparison of data collected at Bordeaux and Cadillac reveals that Cadillac data did not fit any of the relations between settling velocity and SSC obtained with data from Bordeaux. At Cadillac, particles were slightly larger than at Bordeaux (refer to Section 4), which could partly explain the higher settling velocity observed at Cadillac. Such observations seem to indicate a local source of sediment. However, more data are needed to precisely investigate the spatial variability of the settling dynamics. Similarly, van Leussen (1999) also found a variety of relationships linking settling velocity and SSC in the Ems estuary from measurements at five locations. In conclusion, power laws to estimate the settling velocity from SSC were shown to be seasonal and site-specific even in the same estuary.

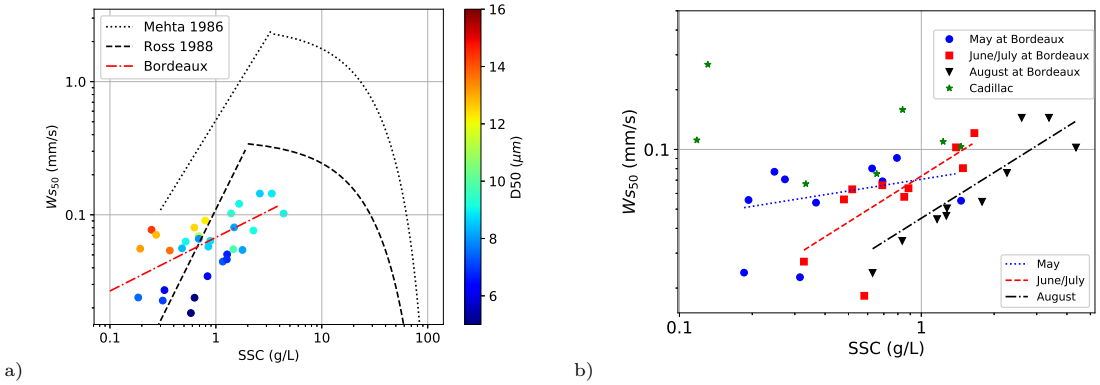

Figure 12: a) Median settling velocity variation with sediment concentration and median diameter. Data collected in surface waters at Bordeaux. b) Median settling velocity variation with sediment concentration for each period of measurement at Bordeaux: May in blue, June/July in green and August in black. Data collected at Cadillac are in red. Data collected in surface waters at Bordeaux.

5.2.2. Relationship with tidal cycle

A variation in the settling velocity throughout the tidal cycle was observed in this study for every condition of tidal (spring/neap tide) and riverine forcing (Fig. 7), suggesting that tidal processes may be one of the major drivers of the settling velocity. Sediment processes and transport mechanisms taking place along the tidal cycle, such as (a) erosion, which resuspends new particles in the water column, increasing the median settling velocity; (b) deposition, during which larger particles settle, decreasing the median settling velocity; and (c) advection, which brings particles from sources other than local, potentially modifying the settling velocity distribution. The counterclockwise hysteresis observed during both flood and ebb tides are similar to those obtained in the Fraser Estuary (Kostaschuk et al., 1989). This lag during the accelerating phase is generally attributed to an enhanced resistance to erosion by bed sediments. In our study, a critical current of 0.4 $m.s^{-1}$ seems to be necessary to resuspend bed sediments, while in the Weser Estuary, a current of 0.2 $m.s^{-1}$ seems to be sufficient to resuspend sediments (Grabemann and Krause, 1989). However, in the Weser Estuary, the u-c relationship does not display a counterclockwise hysteresis, as the measurement site is more affected by advection and depletion than local resuspension and deposition. These different patterns highlight the diversity of the relative importance of advection and mixing on SSC variability in different estuaries even if generic biophysical laws govern fine-scale processes of flocculation and sedimentation. To consider the observed variations in the settling velocity along the tidal cycle in the prediction law for further numerical work, a simple formulation relating the settling velocity to the tidal phase as proposed by Van der Lee (2000) was fitted to the data:

$$ws = a * cos(\frac{2\pi}{T}(t + \phi)) + c \quad (1)$$

where T= 12.4 h is the period of the M2 tidal harmonic (i.e., major harmonic at Bordeaux), t is the time to high water, and a, ϕ and c are constants determined by the fit to the data collected at Bordeaux. The range of settling velocity was estimated to be $a = -0.03\ mm.s^{-1}$, the phase lag to high water was $\phi = 0.25$ hours, and the average settling velocity was determined to be c $= 0.066\ mm.s^{-1}$. This relation is represented in Figure 7 with a full black line. The tidal phase fitted the settling velocity variations only at 41% in a similar manner as the SSC variation. A second formulation was developed taking into consideration the second major tidal harmonic S2 at Bordeaux (Ross and Sottolichio, 2016):

$$ws = a_1 * cos(\frac{2\pi}{T_1}(t + \phi_1)) + a_2 * cos(\frac{2\pi}{T_2}(t + \phi_2)) + c \quad (2)$$

where $a_1 = 0.76\ mm.s^{-1}$, $T_1 = 12.4$ h, $\phi_1 = -0.87$ h, $a_2 = 0.77\ mm.s^{-1}$, $T_2 = 12$ h, $\phi_2 = -0.83$ h, and c $= 0.041\ mm.s^{-1}$. This new formulation better fit the data ($r^2 = 0.56$), as it created a slight asymmetry (Fig. 7 dashed line), and the covariance of the tidal phase and the settling velocity slightly increased with this new formulation (Tab. 2). When discriminating data by periods, the formulation with the two harmonics produced better covariance and better predictive capacity for each period. The predictive capacity of formulations based on tidal phase were better than those obtained with power laws, particularly for data collected in May (i.e., before the arrival of the ETM). Formulation depending on the tidal phase could therefore be more appropriate for numerical simulation once calibrated through campaigns of measurements. In this respect, the

SCAF device offers fast operational readiness and easy handling, in contrast to video systems or LISST instruments.

Table 2: Different formulations for settling velocity prediction

Period	Equation	Covariance	Prediction
all	$ws = 0.068 * SSC^{0.4}$	0.41	0.41
May	$ws = 0.071 * SSC^{0.19}$	0.15	0.05
June/July	$ws = 0.073 * SSC^{0.77}$	0.74	0.74
August	$ws = 0.045 * SSC^{0.77}$	0.69	0.62
all	$ws = -0.03 * cos(2\pi(t + 0.25)/12.4) + 0.066$	0.41	0.41
all	$ws = 0.76 * cos(\frac{2\pi}{12.4}(t - 0.87)) - 0.77 * cos(\frac{2\pi}{12}(t - 0.83)) + 0.041$	0.56	0.56
May	$ws = 0.83 * cos(\frac{2\pi}{12.4}(t - 0.14)) - 0.83 * cos(\frac{2\pi}{12}(t - 0.13)) + 0.03$	0.76	0.57
June/July	$ws = 0.70 * cos(\frac{2\pi}{12.4}(t - 0.84)) - 0.71 * cos(\frac{2\pi}{12}(t - 0.77)) + 0.043$	0.90	0.80
August	$ws = -0.74 * cos(\frac{2\pi}{12.4}(t - 4.22)) + 0.76 * cos(\frac{2\pi}{12}(t + 4.1)) + 0.056$	0.64	0.54

5.3. Comparison to other studies

The settling velocities measured during this study were one order of magnitude lower than the values measured by Manning et al. (2004) at the mouth of the Gironde estuary (1-3 $mm.s^{-1}$) and in other estuaries, such as the Elbe Estuary (Dyer et al., 1996) and the Tamar Estuary (Manning et al., 2006). This could partly be explained by the fact that previous studies generally measured settling velocities close to the bed, where stronger turbulence may resuspend larger particles, and at the mouth of the estuaries, where the bed is mostly composed of sand and salinity may favor flocculation. The order of magnitude difference between the present study and the Manning et al. (2004) study may also come from the different methodology employed: settling column vs. video system, as the video system did not account for the smaller particle size (less than 20 μm). According to Dyer et al. (1996), measurements made with settling columns such as the Owen tube may give settling velocity one order of magnitude smaller than the direct measurement with video systems. In addition, optic systems that rely on isoabsorbances, such as the SCAF instrument, are more sensitive to fine particles, which may lead to underestimation of the settling velocity, as larger flocs are less efficiently considered by such instruments. Coupling different techniques, such as SCAF, video, and laser type, would provide the most efficient strategy. However, settling velocities reported in this work are of the same order of magnitude as those measured in the Yangtze Estuary (Guo et al., 2017) and those measured with natural mud from the Lower Mekong River (Le et al., 2020). This suggests that the findings of this work can be extrapolated to other tidal rivers. For instance, the magnitude and dynamics of the settling velocity can vary significantly between the lower and upper estuary. In tidal rivers, the ETM can play a key role in enhancing flocculation and therefore settling velocities despite the low salinity. The seasonal patterns of the ETM can provide a hint on the seasonal variability of settling velocities in this estuarine region.

Moreover, a similar dependence on tide has been observed for settling velocities in the Dollard Estuary, with a phase lag of the minimum settling velocity of 1 h and 9 min after high water (Van der Lee, 2000). This similarity reinforces the fact that using constant values of settling velocities in a numerical model may not be appropriate, and a better representation of the sediment dynamics

can be given using a settling velocity formulation depending on the tidal phase, particularly in tidal rivers.

6. Conclusion

This study presents the very first values of the settling velocity of cohesive sediments in surface waters measured in the Garonne Tidal River. Settling velocities are hard to measure in situ; however, the new SCAF instrument has shown great potential despite its "quasi in situ" method. The ergonomic and handy design of the SCAF device allows easy-going measurement of settling velocity on a relatively short time scale and in a highly turbid environment. However, the SCAF instrument does not provide information on the size or shape of the particles, which limits data interpretation on floc density. The present results outlined a time and space variability of settling velocities of cohesive sediments. Settling velocity dynamics can vary notably from the lower to upper tidal river. In tidal rivers, settling velocity varies over different time scales. The major variations occur during the tidal cycle, where the median settling velocity of surface sediments may be four times higher at the end of the ebb tide than at high tide. On a longer timescale, ETM may affect settling velocities in two ways: (1) by increasing SSC, which favors flocculation, and (2) by promoting fluid mud in the bed, which modifies the particle size distribution of sediment. In tidal rivers, salinity seems too low to promote flocculation, unlike in lower estuaries. Simple formulations to predict settling velocities are hard to establish due to the large range of influencing factors and their variability in time and space. In the absence of process-based reliable parameterization, a simple empirical formulation based on tidal variation may allow a satisfactory representation of settling velocity and consequently on suspended sediment dynamics in numerical works than with a classical power law related to SSC.

Data in this study are publicly available at https://data.mendeley.com/datasets/6rrzthht5b/1.

7. Acknowledgments

This study was supported by the EMPHASE project (ANR-FRQ). The authors acknowledge Marie-Claire Perello for the Malvern grain-size analysis and Sabine Schmidt for lab support. The authors are grateful to Marine Vandenhove, Maurizio d'Anna, Mario Humbert, Marion Chapalain, Carla Labarthe and Guillaume Detandt for their support during fieldwork.

Abril, G., Nogueira, M., Etcheber, H., Cabeçadas, G., Lemaire, E., Brogueira, M., 2002. Behaviour of organic carbon in nine contrasting european estuaries. Estuarine, coastal and shelf science 54, 241–262.

Agrawal, Y.C., Pottsmith, H.C., 2000. Instruments for particle size and settling velocity observations in sediment transport. Marine Geology 168, 89–114.

Allen, G.P., 1971. Relationship between grain size parameter distribution and current patterns in the gironde estuary (france). Journal of Sedimentary Research 41, 74–88.

Allen, G.P., Salomon, J., Bassoullet, P., Du Penhoat, Y., De Grandpre, C., 1980. Effects of tides on mixing and suspended sediment transport in macrotidal estuaries. Sedimentary Geology 26, 69–90.

Bonneton, P., Bonneton, N., Parisot, J.P., Castelle, B., 2015. Tidal bore dynamics in funnel-shaped estuaries. Journal of Geophysical Research: Oceans 120, 923–941.

Boss, E., Slade, W., Hill, P., 2009. Effect of particulate aggregation in aquatic environments on the beam attenuation and its utility as a proxy for particulate mass. Optics express 17, 9408–9420.

Burchard, H., Schuttelaars, H.M., Ralston, D.K., 2018. Sediment trapping in estuaries. Annual review of marine science 10, 371–395.

Cornelisse, J.M., 1996. The field pipette withdrawal tube (fipiwitu). Journal of Sea Research 36, 37–39.

Deng, Z., He, Q., Chassagne, C., Wang, Z.B., 2021. Seasonal variation of floc population influenced by the presence of algae in the changjiang (yangtze river) estuary. Marine Geology 440, 106600.

Diaz, M., Grasso, F., Le Hir, P., Sottolichio, A., Caillaud, M., Thouvenin, B., 2020. Modeling mud and sand transfers between a macrotidal estuary and the continental shelf: Influence of the sediment transport parameterization. Journal of Geophysical Research: Oceans 125, e2019JC015643.

Downing, J., 2006. Twenty-five years with obs sensors: The good, the bad, and the ugly. Continental Shelf Research 26, 2299–2318.

Druine, F., Verney, R., Deloffre, J., Lemoine, J.P., Chapalain, M., Landemaine, V., Lafite, R., 2018. In situ high frequency long term measurements of suspended sediment concentration in turbid estuarine system (seine estuary, france): Optical turbidity sensors response to suspended sediment characteristics. Marine Geology 400, 24–37.

Dyer, K., Cornelisse, J., Dearnaley, M., Fennessy, M., Jones, S., Kappenberg, J., McCave, I., Pejrup, M., Puls, W., Van Leussen, W., et al., 1996. A comparison of in situ techniques for estuarine floc settling velocity measurements. Journal of Sea Research 36, 15–29.

Dyer, K., Manning, A., 1999. Observation of the size, settling velocity and effective density of flocs, and their fractal dimensions. Journal of sea research 41, 87–95.

Eisma, D., 1986. Flocculation and de-flocculation of suspended matter in estuaries. Netherlands Journal of sea research 20, 183–199.

Eisma, D., Bernard, P., Cadee, G., Ittekkot, V., Kalf, J., Laane, R., Martin, J.M., Mook, W., Van Put, A., Schuhmacher, T., 1991. Suspended-matter particle size in some west-european estuaries; part i: Particle-size distribution. Netherlands journal of sea research 28, 193–214.

Etcheber, H., Taillez, A., Abril, G., Garnier, J., Servais, P., Moatar, F., Commarieu, M.V., 2007. Particulate organic carbon in the estuarine turbidity maxima of the gironde, loire and seine estuaries: origin and lability. Hydrobiologia 588, 245–259.

Fall, K.A., Friedrichs, C.T., Massey, G.M., Bowers, D.G., Smith, S.J., 2021. The importance of organic content to fractal floc properties in estuarine surface waters: Insights from video, lisst, and pump sampling. Journal of Geophysical Research: Oceans 126, e2020JC016787.

Fennessy, M., Dyer, K., Huntley, D., 1994. Inssev: An instrument to measure the size and settling velocity of flocs in situ. Marine geology 117, 107–117.

Furukawa, Y., Reed, A.H., Zhang, G., 2014. Effect of organic matter on estuarine flocculation: a laboratory study using montmorillonite, humic acid, xanthan gum, guar gum and natural estuarine flocs. Geochemical Transactions 15, 1–9.

Gibbs, R., Tshudy, D., Konwar, L., Martin, J.M., 1989. Coagulation and transport of sediments in the gironde estuary. Sedimentology 36, 987–999.

Gibbs, R.J., 1983. Coagulation rates of clay minerals and natural sediments. Journal of Sedimentary Research 53, 1193–1203.

Grabemann, I., Krause, G., 1989. Transport processes of suspended matter derived from time series in a tidal estuary. Journal of Geophysical Research: Oceans 94, 14373–14379.

Graham, G.W., Nimmo Smith, W.A.M., 2010. The application of holography to the analysis of size and settling velocity of suspended cohesive sediments. Limnology and Oceanography: Methods 8, 1–15.

Gratiot, N., Coulaud, C., Legout, C., Mercier, B., Mora, H., Wendling, V., 2015. Unit for measuring the falling speed of particles in suspension in a fluid and device comprising at least one measuring unit and one automatic sampler. Patent-Publication number WO2015055963 A 1.

Gratiot, N., Manning, A., 2004. An experimental investigation of floc characteristics in a diffusive turbulent flow. Journal of Coastal Research , 105–113.

Guo, C., He, Q., Guo, L., Winterwerp, J.C., 2017. A study of in-situ sediment flocculation in the turbidity maxima of the yangtze estuary. Estuarine, Coastal and Shelf Science 191, 1–9.

Heffler, D., Syvitski, J., Asprey, K., 1991. The floc camera. Principles, methods, and application of particle size analysis , 209–221.

Horemans, D.M., Dijkstra, Y.M., Schuttelaars, H.M., Meire, P., Cox, T.J., 2020. Unraveling the essential effects of flocculation on large-scale sediment transport patterns in a tide-dominated estuary. Journal of Physical Oceanography 50, 1957–1981.

Jalón Rojas, I., 2016. Évaluation des changements hydro-sédimentaires de l'estuaire de la Gironde en lien avec les pressions sur le milieu. Ph.D. thesis. Bordeaux.

Jalón-Rojas, I., Dijkstra, Y., Schuttelaars, H., Brouwer, R., Schmidt, S., Sottolichio, A., 2021. Multidecadal evolution of the turbidity maximum zone in a macrotidal river under climate and anthropogenic pressures. Journal of Geophysical Research: Oceans 126, e2020JC016273.

Jalón-Rojas, I., Schmidt, S., Sottolichio, A., 2015. Turbidity in the fluvial gironde estuary (south-west france) based on 10-year continuous monitoring: sensitivity to hydrological conditions. Hydrology and Earth System Sciences 19, 2805–2819.

Jalón-Rojas, I., Sottolichio, A., Hanquiez, V., Fort, A., Schmidt, S., 2018. To what extent multi-decadal changes in morphology and fluvial discharge impact tide in a convergent (turbid) tidal river. Journal of Geophysical Research: Oceans 123, 3241–3258.

Jones, S., Jago, C., 1996. Determination of settling velocity in the elbe estuary using quisset tubes. Journal of Sea Research 36, 63–67.

Kineke, G., Sternberg, R., Johnson, R., 1989. A new instrument for measuring settling velocities in situ. Marine Geology 90, 149–158.

Kostaschuk, R., Luternauer, J., Church, M., 1989. Suspended sediment hysteresis in a salt-wedge estuary: Fraser river, canada. Marine Geology 87, 273–285.

Lajaunie-Salla, K., Wild-Allen, K., Sottolichio, A., Thouvenin, B., Litrico, X., Abril, G., 2017. Impact of urban effluents on summer hypoxia in the highly turbid gironde estuary, applying a 3d model coupling hydrodynamics, sediment transport and biogeochemical processes. Journal of Marine Systems 174, 89–105.

Le, H.A., Gratiot, N., Santini, W., Ribolzi, O., Tran, D., Meriaux, X., Deleersnijder, E., Soares-Frazão, S., 2020. Suspended sediment properties in the lower mekong river, from fluvial to estuarine environments. Estuarine, Coastal and Shelf Science 233, 106522.

Van der Lee, W.T., 2000. Temporal variation of floc size and settling velocity in the dollard estuary. Continental Shelf Research 20, 1495–1511.

Legout, C., Droppo, I., Coutaz, J., Bel, C., Jodeau, M., 2018. Assessment of erosion and settling properties of fine sediments stored in cobble bed rivers: the arc and isère alpine rivers before and after reservoir flushing. Earth Surface Processes and Landforms 43, 1295–1309.

van Leussen, W., 1996. The rws field settling tube. Journal of Sea Research 36, 83–86.

van Leussen, W., 1999. The variability of settling velocities of suspended fine-grained sediment in the ems estuary. Journal of sea research 41, 109–118.

Liu, D., Edraki, M., Berry, L., 2018. Investigating the settling behaviour of saline tailing suspensions using kaolinite, bentonite, and illite clay minerals. Powder Technology 326, 228–236.

van Maanen, B., Sottolichio, A., 2018. Hydro-and sediment dynamics in the gironde estuary (france): Sensitivity to seasonal variations in river inflow and sea level rise. Continental Shelf Research 165, 37–50.

Malarkey, J., Baas, J.H., Hope, J.A., Aspden, R.J., Parsons, D.R., Peakall, J., Paterson, D.M., Schindler, R.J., Ye, L., Lichtman, I.D., et al., 2015. The pervasive role of biological cohesion in bedform development. Nature communications 6, 1–6.

Manning, A., Dyer, K., 2007. Mass settling flux of fine sediments in northern european estuaries: measurements and predictions. Marine Geology 245, 107–122.

Manning, A., Dyer, K., Lafite, R., Mikes, D., 2004. Flocculation measured by video based instruments in the gironde estuary during the european commission swamiee project. Journal of Coastal Research , 58–69.

Manning, A., Friend, P., Prowse, N., Amos, C., 2007. Estuarine mud flocculation properties determined using an annular mini-flume and the labsfloc system. Continental Shelf Research 27, 1080–1095.

Manning, A., Schoellhamer, D.H., 2013. Factors controlling floc settling velocity along a longitudinal estuarine transect. Marine Geology 345, 266–280.

631 Manning, A.J., Bass, S.J., Dyer, K.R., 2006. Floc properties in the turbidity maximum of a
632 mesotidal estuary during neap and spring tidal conditions. Marine Geology 235, 193–211.

633 Manning, A.J., Baugh, J.V., Spearman, J.R., Whitehouse, R.J., 2010. Flocculation settling char-
634 acteristics of mud: sand mixtures. Ocean dynamics 60, 237–253.

635 Mantovanelli, A., 2005. A new approach for measuring in situ the concentration and settling velocity
636 of suspended cohesive sediment. Ph.D. thesis. James Cook University.

637 Mantovanelli, A., Ridd, P.V., 2006. Devices to measure settling velocities of cohesive sediment
638 aggregates: A review of the in situ technology. Journal of Sea Research 56, 199–226.

639 Mehta, A.J., 1986. Characterization of cohesive sediment properties and transport processes in
640 estuaries, in: Estuarine cohesive sediment dynamics. Springer, pp. 290–325.

641 Mehta, A.J., 2013. An introduction to hydraulics of fine sediment transport. volume 38. World
642 Scientific Publishing Company.

643 Mietta, F., Chassagne, C., Manning, A.J., Winterwerp, J.C., 2009. Influence of shear rate, organic
644 matter content, ph and salinity on mud flocculation. Ocean Dynamics 59, 751–763.

645 Mikeš, D., Manning, A.J., 2010. Assessment of flocculation kinetics of cohesive sediments from the
646 seine and gironde estuaries, france, through laboratory and field studies. Journal of Waterway,
647 Port, Coastal, and Ocean Engineering 136, 306–318.

648 Mikes, D., Verney, R., Lafite, R., Belorgey, M., 2004. Controlling factors in estuarine flocculation
649 processes: experimental results with material from the seine estuary, northwestern france. Journal
650 of coastal research , 82–89.

651 Mikkelsen, O., Pejrup, M., 1998. Comparison of flocculated and dispersed suspended sediment in
652 the dollard estuary. Geological Society, London, Special Publications 139, 199–209.

653 Mikkelsen, O., Pejrup, M., 2001. The use of a lisst-100 laser particle sizer for in-situ estimates of
654 floc size, density and settling velocity. Geo-Marine Letters 20, 187–195.

655 Murray, P., McCave, I., Owen, T., Mason, M., Green, M., 1996. A robust in situ settling velocity
656 box for coastal seas. Journal of Sea Research 36, 101–107.

657 Owen, M., 1971. The effect of turbulence on the settling velocities of silt flocs, in: Proceedings of
658 the Fourteenth Congress of IAHR, pp. 27–32.

659 Owen, R.B., Zozulya, A.A., 2000. In-line digital holographic sensor for monitoring and character-
660 izing marine particulates. Optical Engineering 39, 2187–2197.

661 Parsons, D.R., Schindler, R.J., Hope, J.A., Malarkey, J., Baas, J.H., Peakall, J., Manning, A.J., Ye,
662 L., Simmons, S., Paterson, D.M., et al., 2016. The role of biophysical cohesion on subaqueous
663 bed form size. Geophysical research letters 43, 1566–1573.

664 Pejrup, M., 1988. Flocculated suspended sediment in a micro-tidal environment. Sedimentary
665 Geology 57, 249–256.

Pejrup, M., Edelvang, K., 1996. Measurements of in situ settling velocities in the elbe estuary. Journal of Sea Research 36, 109–113.

Pejrup, M., Mikkelsen, O.A., 2010. Factors controlling the field settling velocity of cohesive sediment in estuaries. Estuarine, Coastal and Shelf Science 87, 177–185.

Piro, P., Carbone, M., Penna, N., Marsalek, J., 2011. Characterization of the settling process for wastewater from a combined sewer system. Water research 45, 6615–6624.

Puls, W., Kuehl, H., Heymann, K., 1988. Settling velocity of mud flocs: results of field measurements in the elbe and the weser estuary, in: Physical processes in estuaries. Springer, pp. 404–424.

Puls, W., Kühl, H., 1996. Settling velocity determination using the bigdan settling tube and the owen settling tube. Journal of Sea Research 36, 119–125.

Ross, L., Sottolichio, A., 2016. Subtidal variability of sea level in a macrotidal and convergent estuary. Continental Shelf Research 131, 28–41.

Ross, M.A., 1988. Vertical structure of estuarine fine sediment suspension. Ph. D. Thesis, Coastal and Oceanographic Eng. Department, University of Florida .

Sanford, L., Dickhudt, P., Rubiano-Gomez, L., Yates, M., Suttles, S., Friedrichs, C., Fugate, D., Romine, H., 2005. Variability of suspended particle concentrations, sizes, and settling velocities in the chesapeake bay turbidity maximum. Flocculation in natural and engineered environmental systems , 211–236.

SEQUOIA, . LISST-HOLO 2, SUBMERSIBLE DIGITAL HOLOGRAPHIC CAMERA.

Smith, S.J., Friedrichs, C.T., 2011. Size and settling velocities of cohesive flocs and suspended sediment aggregates in a trailing suction hopper dredge plume. Continental Shelf Research 31, S50–S63.

Sottolichio, A., Castaing, P., 1999. A synthesis on seasonal dynamics of highly-concentrated structures in the gironde estuary. Comptes Rendus de l'Académie des Sciences-Series IIA-Earth and Planetary Science 329, 795–800.

Sottolichio, A., Hurther, D., Gratiot, N., Bretel, P., 2011. Acoustic turbulence measurements of near-bed suspended sediment dynamics in highly turbid waters of a macrotidal estuary. Continental Shelf Research 31, S36–S49.

Soulsby, R., Manning, A., Spearman, J., Whitehouse, R., 2013. Settling velocity and mass settling flux of flocculated estuarine sediments. Marine Geology 339, 1–12.

Spearman, J.R., Manning, A.J., Whitehouse, R.J., 2011. The settling dynamics of flocculating mud and sand mixtures: part 2—numerical modelling. Ocean Dynamics 61, 351–370.

Stein, R., 1985. Rapid grain-size analyses of clay and silt fraction by sedigraph 5000d: comparison with coulter counter and atterberg methods. Journal Of Sedimentary Research 55.

Sternberg, R., Ogston, A., Johnson, R., 1996. A video system for in situ measurement of size and settling velocity of suspended particulates. Journal of Sea Research 36, 127–130.

Van Leussen, W., Cornelisse, J.M., 1993. The determination of the sizes and settling velocities of estuarine flocs by an underwater video system. Netherlands Journal of Sea Research 31, 231–241.

Verney, R., Lafite, R., Brun-Cottan, J.C., 2009. Flocculation potential of estuarine particles: The importance of environmental factors and of the spatial and seasonal variability of suspended particulate matter. Estuaries and coasts 32, 678–693.

Verney, R., Lafite, R., Brun-Cottan, J.C., Le Hir, P., 2011. Behaviour of a floc population during a tidal cycle: Laboratory experiments and numerical modelling. Continental Shelf Research 31, S64–S83.

Watson, J., Chalvidan, V., Chambard, J., Craig, G., Diard, A., Foresti, G., Forre, B., Gentili, S., Hobson, P., Lampitt, R., Maine, P., et al., 1998. High-resolution in situ holographic recording and analysis of marine organisms and particles (holomar), in: IEEE Oceanic Engineering Society. OCEANS'98. Conference Proceedings (Cat. No. 98CH36259), IEEE. pp. 1599–1603.

Watson, J., Player, M., Sun, H., Hendry, D., Dong, H., 2004. eholocam-an electronic holographic camera for subsea analysis, in: Oceans' 04 MTS/IEEE Techno-Ocean'04 (IEEE Cat. No. 04CH37600), IEEE. pp. 1248–1254.

Wendling, V., 2015. Développement d'un système de caractérisation des agrégats et des flocs en suspension. Ph.D. thesis. Université Grenoble Alpes.

Wendling, V., Gratiot, N., Legout, C., Droppo, I.G., Coulaud, C., Mercier, B., 2015. Using an optical settling column to assess suspension characteristics within the free, flocculation, and hindered settling regimes. Journal of Soils and Sediments 15, 1991–2003.

Whitehouse, R., Soulsby, R., Roberts, W., Mitchener, H., 2000. Dynamics of estuarine muds. Thomas Telford Publishing.

Winterwerp, J., Manning, A., Martens, C., De Mulder, T., Vanlede, J., 2006. A heuristic formula for turbulence-induced flocculation of cohesive sediment. Estuarine, Coastal and Shelf Science 68, 195–207.

Winterwerp, J.C., 2002. On the flocculation and settling velocity of estuarine mud. Continental shelf research 22, 1339–1360.

Xia, X., Li, Y., Yang, H., Wu, C., Sing, T., Pong, H., 2004. Observations on the size and settling velocity distributions of suspended sediment in the pearl river estuary, china. Continental Shelf Research 24, 1809–1826.

Xu, F., Wang, D.P., Riemer, N., 2010. An idealized model study of flocculation on sediment trapping in an estuarine turbidity maximum. Continental Shelf Research 30, 1314–1323.

Zaneveld, J.R.V., Spinrad, R.W., Bartz, R., 1982. An optical settling tube for the determination of particle-size distributions. Marine Geology 49, 357–375.

Zhang, Y., Ren, J., Zhang, W., Wu, J., 2021. Importance of salinity-induced stratification on flocculation in tidal estuaries. Journal of Hydrology 596, 126063.